# Dissociative Multiple Photoionization of $GeCl_4$: The Ge(3d,3p,3s) and Cl(2p,2s) Inner-Shell Excitation in the Range 88∼1006 eV

**Bong Hyun Boo,*,† Jae Kwang Lee,† and Norio Saito‡**

*Department of Chemistry, Chungnam National University, Daejeon 305-764, South Korea, and Electrotechnical Laboratory, 1-1-4, Umezono, Tsukuba-shi, Ibaraki 305, Japan*

*Received: August 8, 2001; In Final Form: November 5, 2001*

The dissociative multiple photoionization of germanium tetrachloride ($GeCl_4$) in the Ge(3d,3p,3s) and Cl(2p,2s) inner-shell regions has been studied by using time-of-flight (TOF) mass spectrometry coupled to synchrotron radiation in the range 88∼1006 eV. Total and individual photoion yields have been recorded as a function of the incident photon energy. Discrete resonances owing to the Ge(3p) → $(9a_1)$* and the Ge(3s) → $(11t_2)$* transitions are observed as doublet and singlet features, respectively. The inner-shell excitation spectrum is dominated by overlapped numerous discrete resonances of the Cl(2p) inner-shell electron, arising from the large overlap of the valence state wave function with the initial inner-shell state one. Prominent ion intensities of $Cl^+$, $Ge^+$, and $GeCl^+$ are detected along with low-intensity $Cl^{2+}$, $GeCl^{2+}$, and $GeCl_n^+$ ($n$ = 2−4) ions in the whole energy range examined. Dissociation processes have also been investigated by photoelectron−photoion coincidence (PEPICO) and photoion−photoion coincidence (PIPICO) methods. The triple and quadruple photoionization of $GeCl_4$ is found to dominantly occur above the Cl(2p) edge, leading to the exclusive formation of the $GeCl_n^+$ ($n$ = 0, 1) + $n$$Cl^+$ ($n$ = 2−3) channels.

## Introduction

Inner-shell excitation is an attractive tool with respect to the problem of site-specific excitation and decay leading to the site-selective photochemistry, which eventually enables us to evaluate geometric and electronic structures of molecules.[1] This site-selectivity in the photochemistry largely relies on how long for the localization of excess energy resulting from core excitation to reside in a specific atom and its neighbor for the corresponding bond breakage, competing with energy and charge redistribution in the molecule. Therefore the elucidation concerning charge and energy redistribution following the core excitation/ionization provides an insight into the energy dissipation processes such as Auger process and bond cleavage of the core-excited molecule.

Studies of the fragmentation pathways in dissociative multiple ionization of a molecule involve a variety of coincidence methods such as photoelectron−photoion (PEPICO), photoion−photoion (PIPICO), and photoelectron−photoion−photoion (PEPIPICO, PE2PICO) coincidence.[2] Among these, the triple coincidence PEPIPICO method was proven to be a powerful tool to elucidate the dynamics in dissociative double ionization processes.[3−5] Recent addition of position-sensitive ion detection technology to the existing PEPICO spectroscopic tool in the PEPIPICO method enables us to investigate angle-resolved product distribution in the dissociation of doubly charged ions by using a two-dimensional imaging process.[4,6] Until now, however, the PEPIPICO method is almost confined to the investigation of the three-body dissociation dynamics of relatively small dications.

Hydrogen,[7,8] carbon(IV),[9] phosphorus(III),[10] and germanium(IV) chorides[11,12] together with atomic chlorine[13,14] have been the subject of photoabsorption and photoionization in the X-ray region. These studies have demonstrated that the photoionization cross sections (or yields or differential oscillator strength) in the energy range above the Cl(2p) threshold are dominated by strong lines of overlapped numerous discrete resonances due to the Cl(2p,2s) excitations, which are similar to each other in shape and strength, but showing some shift in the energy dependence of the photoionization cross section.

For a probe of competition between electronic relaxation and photochemical degradation of the core−hole state, we have chosen the $GeCl_4$ molecule in which the central Ge atom is surrounded by strongly electronegative chlorine atoms which can create an effective potential barrier, and consequently the large overlap between the valence state wave function and the initial inner-shell state could give rise to strongly enhanced spectral features.[10,15,16] Although the previous ab initio studies and X-ray absorption, inner-shell electron energy loss, electron transmission, and dissociative electron attachment spectroscopic studies of $GeCl_4$ [11,12] by Guillot et al. are quite informative as to the photoabsorption positions and spectral features of the various core−hole states, additional information on the relative importance of individual ions in the photoionization is necessary to derive individual photoionization cross sections. Furthermore, study of dissociation processes associated with various discrete core excitation channels could become a viable approach to the understanding of the core ionization structure.

In this report, we were concerned about the discrete excitation and the subsequent critical fragmentation phenomena involving the Ge(3d,3p,3s) and Cl(2p,2s) inner-shell excitations in the range 88−1006 eV. Various dissociation patterns of the multiply charged parent ions are proposed on the basis of the measurements of the ion TOF differences in the PIPICO mode. Comparison of the dissociation patterns was made in the Ge(3p,3s) and Cl(2p,2s) core excitation regions, and the congruent effect of the valence ionization and core-excitation/ionization on the ionic photodissociation are elucidated.

## Experimental Section

Monochromatic vacuum ultraviolet and soft X-rays were obtained by dispersing synchrotron radiation from the TERAS

* Author to whom correspondence should be addressed. Fax: 82-42-823-1360. E-mail: bhboo@cuvic.cnu.ac.kr.
† Chungnam National University.
‡ Electrotechnical Laboratory.

10.1021/jp0130970 CCC: $22.00 
Published on Web 01/29/2002

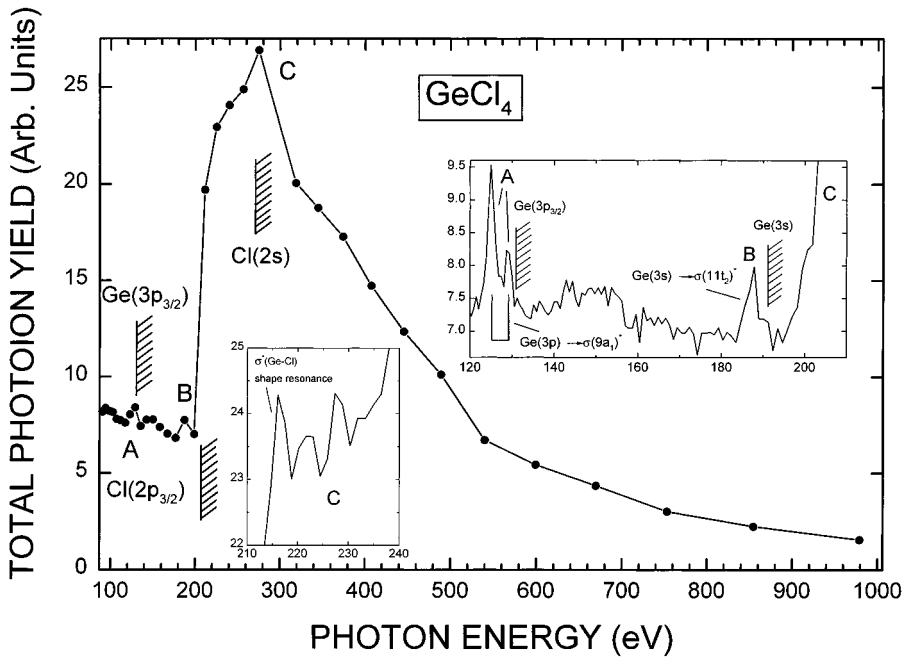


**Figure 1.** Total photoion yield of $GeCl_4$. The insets show the scale-expanded spectrum measured specifically for the Ge(3p) and Cl(2p) regions in the short range.

storage ring at the Electrotechnical Laboratory using a Grasshopper monochromator. The principle and construction of the whole apparatus have been described in detail elsewhere,[17,18] and thus only briefly described here. The monochromatized photons pass through two differential pumping stages and entered an ionization chamber equipped with a TOF spectrometer. Here an electric field of 142.9 V/cm was applied to the ionization chamber for ion and electron extraction. The main chamber where the ionization cell, a photoelectron detector, and the TOF spectrometer were equipped was evacuated down to $\approx 6 \times 10^{-7}$ Torr. When the $GeCl_4$ gas molecules were introduced into the ionization cell, the pressure of the main chamber was maintained at $\approx 4 \times 10^{-5}$ Torr. The flight path length was 13 cm and the mass detection angle was perpendicular to the direction of incident photon beam and 55° to the photon beam polarization. The uncertainty in the photon beam energy lies within ±0.1 eV.

The total ion yield spectrum was obtained by recording the count rates of the total ions and the photon intensities simultaneously while the photon wavelength is scanned. For characterization of individual ions and ion pairs, the time-correlated ion counting technique was used in the two modes of PEPICO and PIPICO, respectively. The PEPICO mode utilizes the start pulses for a time-to-amplitude converter (TAC) provided by the photoelectron arrival signals at a microchannel plate (MCP), sampled from the collision chamber in the opposite direction to the ion flight direction, and the stop pulses are generated by the photoion detection signals at another MCP located at the end of the TOF tube. However, the PIPICO mode uses the start pulses provided by the lighter ions, here $Cl^+$ ions, and the stop pulses are generated by the heavier ions of the counterparts. Similarly the total PIPICO yield spectrum was obtained by measuring the count rates of total PIPICO simultaneously while the photon wavelength is scanned. For the measurements of the PIPICO count rates, the coincidence time range (gate width in TAC) was set to be 0−10 μs, because the TOF difference between any pairs of ions formed from $GeCl_4$ is found to fall into this time range. The individual ion and PIPICO yields at a photon energy were obtained by multiplying the individual ion and PIPICO intensity ratios measured in the coincidence mode by the total ion and PIPICO yields, respectively.

The corrected photon intensities were obtained by dividing the measured photoemission yields from a gold mesh photocathode placed between the exit slit of the monochromator and the experimental main chamber by the published photoemission efficiency of a gold photocathode.[19] Relative uncertainties in the normalized ion and PIPICO yields may mainly come from this normalization process and could be estimated as less than ≈10%. The sample $GeCl_4$ with a nominal purity of 99.99% was purchased from Aldrich Chemical Co. and used without further purification.

## Results and Discussion

**A. Core Excitation Spectra.** Figure 1 presents the total photoion yield of $GeCl_4$ vs the photon energy in the range 88−1006 eV. It is noticed that some of literature values for the thresholds of the various core electrons are indicated with hatched lines over the photoionization yield curve of $GeCl_4$, the thresholds of the core electrons for $GeCl_4$ are the following: $Ge(3d_{5/2}) = 40.07 \pm 0.05$ eV[20] and 40.10 eV;[21] $Ge(3p_{3/2}) = 132.12$ eV[21] and 131.98 eV;[22] Ge(3s) = 191.4 eV, the value estimated by Guillot et al.;[11] $Cl(2p_{3/2}) = 206.70 \pm 0.05$ eV[21] and 206.70 eV.[20] That for atomic chlorine is Cl(2s) = 270 eV.[23] Here we have observed a prominent doublet feature (peak A) at 125.0 and 129.0 eV, peak B at 187.9 eV, and a broad peak C beginning about 196 eV.

**Ge(3p) and Ge(3s) Regions.** The transition below ≈132 eV (peak A) is attributed to the excitation of the $Ge(3p_{3/2})$ and $Ge(3p_{1/2})$ core electrons to the unoccupied antibonding orbitals. The peak width 4.0 eV is in excellent agreement with a reported spin−orbit splitting value 4.1 eV in $GeCl_4$,[12] and consistent with 4.3 eV in $Ge(CH_3)_4$,[24] and a little lower than that of $GeH_4 \approx$ 5.0 eV.[25] It is apparent that the $Ge(3p_{3/2})$ excitation is almost twice as intense as the $Ge(3p_{1/2})$ one, correctly reflecting the statistical ratio for the $Ge(3p_{3/2})$ and $Ge(3p_{1/2})$ spin−orbit population. From the reported ionization energy (IE), 132.12 eV[21] and the core−hole excited-state energy (*E*) determined

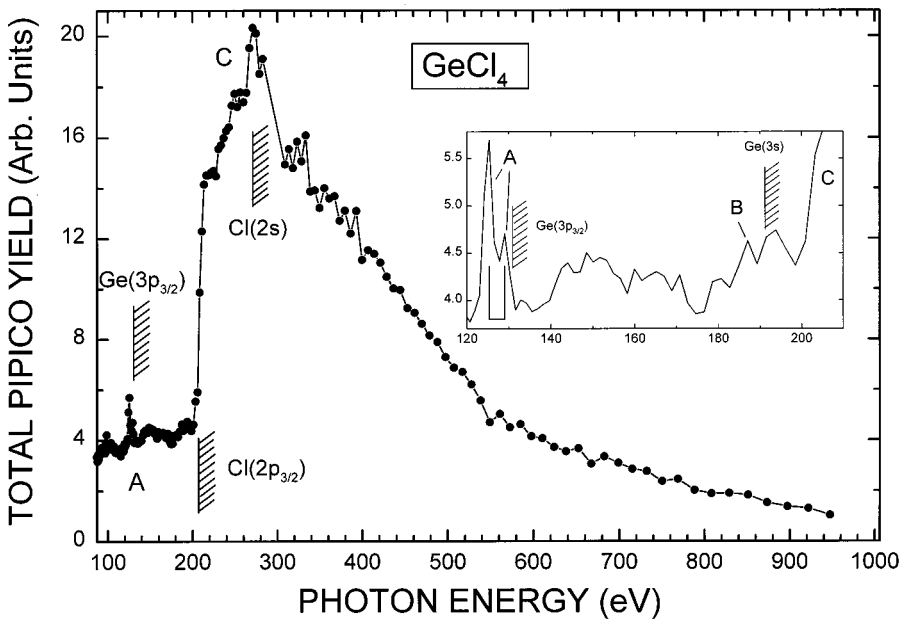


**Figure 2.** Total photoion−photoion yield of $GeCl_4$. The inset shows the scale-expanded spectrum spanning the Ge(3p) and Cl(2p) regions.

here, 125.0 eV, the term value (TV) of the Ge($3p_{3/2}$) core−hole state in $GeCl_4$ [*IE* (Ge($3p_{3/2}$)) − *E*(Ge($3p_{3/2}$))] is determined as 7.1 eV, being lower than that for the Ge($2p_{3/2}$) 8.8 eV, the value estimated for $GeCl_4$ by Guillot et al.[12] The discrepancy may come from one possibility that the Ge(3p) electron could not shield the Ge nuclear charge completely as the Ge(2p) electron could, the TV of which is evaluated for the Ge($2p_{3/2}$) core−hole state by Guillot.[12]

The peak at 187.9 eV (peak B) may correspond to the discrete resonance of the Ge(3s) → $\sigma(11t_2)$* below the Ge(3s) threshold.[11] It should be noticed that the Ge(3s) → $\sigma(9a_1)$* transition is symmetry-forbidden in the $T_d$ symmetry while the transition to $\sigma(11t_2)$* is dipole-allowed. This confirms that the Ge(3s) prethreshold feature (Figures 1 and 2) corresponds to the Ge(3s) → $\sigma(11t_2)$* transition. Here the term value for the Ge(3s) core−hole state is estimated as 3.5 eV, being less than the reported term value of 4.8 eV.[12] Not surprisingly, Rydberg series corresponding to the Ge(3p) and Ge(3s) excitations are not observed, being consistent with a previous observation in the photoabsorption of $PCl_3$,[10,16] in which the stronger transitions to the $\sigma$* than to the Rydberg orbitals occur because of the slight overlap between the Rydberg state wave function and the initial inner-shell state one.[10,15,16] The pre-edge features corresponding to the Ge(3p,3s) → $\sigma$* transitions in the Ge(3p,3s) spectra arise from the presence of the electronegative chlorine ligand, which gives rise to the backscattering of the escaping photoelectron.[15,16] This strong repulsive force acting on the escaping electron would bring about an effective potential barrier, which separates the molecular field into an inner-well region in which the virtual valence excited-state resides, as well as an outer-well region, in which Rydberg state is located. Therefore the wave function overlap between the Rydberg state and initial inner-shell state is small.

Figure 2 presents the total PIPICO yield curve for comparison with the total ion yield curve. The shape of the total PIPICO yield spectrum looks similar for that of the total ion yield spectrum. Here the doublet feature at 125.4 and 129.0 eV (peak A) and the broad and enormous feature (Peak C) also appear, indicating that the resonance excitations end up with the formation of the various ion-pairs to yield the high PIPICO intensity. It is noticed that the spin−orbit separation due to the Ge(3p) excitation in the PIPICO yield curve (Figure 2) is 3.6 eV, a little lower than that in the ion yield curve (Figure 1). This may happen simply because fewer data points (Figure 2) were obtained in the PIPICO yield measurement than those in the total yield measurement (Figure 1).

**Cl(2p,2s) Regions.** As seen in Figures 1 and 2, photoionization efficiency due to the Cl(2p) excitation is greatly enhanced, in comparison with that observed in HCl molecule.[7,8] This is because in $GeCl_4$, the central Ge atom is surrounded by the four electronegative atoms which can create an effective potential barrier by which antibonding orbital and/or quasibound unoccupied orbitals are supported. In the potential well, the excited electron could be backscattered by the chlorine ligands, which gives rise to a shape resonance above the threshold. The large overlap between the valence state wave function and the initial inner-shell state gives rise to strongly enhanced spectral features. On the basis of the theoretical[7] and experimental[8] treatments, the huge peak rising steeply about 196 eV, the energy near the Cl($2p_{3/2}$) = 206.70 ± 0.05 eV, can be interpreted as being due to overlapped numerous discrete resonances corresponding to the transitions of the inner-shell orbitals of the Cl($2p_{3/2}$) and Cl($2p_{1/2}$) to the $\sigma$* valence orbitals and the *n*s and *n*p Rydberg series. The peak at 216.1 eV in the inset shown in Figure 1 is assigned as the $\sigma$*(Ge−Cl) shape resonance arising from potential barrier effect caused by the electronegative chlorine ligands.[12,15] Even far beyond the Cl(2s) threshold, the intensity of peak C is not diminished steeply, having a shoulder up to ≈500 eV. The broad absorption after the Cl(2s) threshold observed in Figures 1 and 2 may mainly come from a shake-off process, in which a fast electron is ejected involving simultaneous loss of one more electron, and thus multiple photoionization prevails in the shake-off process. Therefore more ions with lighter masses such as $Cl^+$, $Ge^+$, and $GeCl^+$ are dominantly formed in the shake-off region.

**B. Dissociation Behaviors.** Figure 3 shows TOF mass spectra taken in the PEPICO mode at 88, 110, 130, 190, 210, 285, 500, and 900 eV, where the core orbitals are marked below the energies of the photon utilized, by which the deepest core orbitals could be excited or ionized. Various monocations of

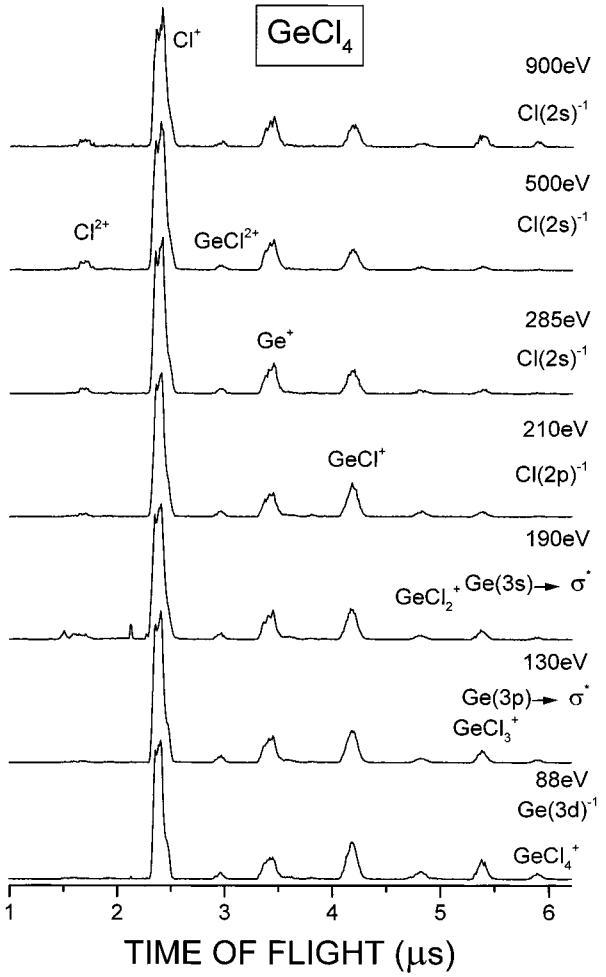


**Figure 3.** Photoelectron and photoion coincidence (mass) spectra of $GeCl_4$ taken by excitations at photon energies at 88, 130, 190, 160, 210, 285, 500, and 900 eV. The deepest core orbitals, which could be excited/ionized by the specified energy, are marked in the individual spectra.

$Cl^{2+}$, $Cl^+$, $GeCl^{2+}$, $Ge^+$, $GeCl^+$, $GeCl_2^+$, $GeCl_3^+$, and $GeCl_4^+$ are observed in the whole energy range. The energy of 88 eV, the lowest energy examined, corresponds to the valence and the Ge(3d) core excitation regions in which various monocations with the higher masses are formed in relatively large amounts. This is because in the nonresonant valence ionization processes, sufficient energy to break all the Ge−Cl bonds completely is not left relatively in the parent ion. In the excitation above 210 eV, however, relatively sufficient energy could be stored in a molecule leading to the cleavage of all the Ge−Cl bonds. Even at high energies above the Cl(2p) threshold, singly charged ions such as $Ge^+$ and $GeCl^+$ are still dominant. This implies that the dissociation partners for the $GeCl_n^+$ ($n = 0-1$) ions could take away excess energy from the parent ions, and thus the resulting $GeCl_n^+$ ($n = 0-1$) ions could be stabilized without being involved in further loss of electrons.

Figure 4 shows the variation of the partial ion yields with energy, which were derived on the basis of the photon intensity utilized for the determination of the individual ion yields. It is noticed that sum of the individual ion yields equals to the total ion yield as shown in Figure 1. Figure 5 presents PIPICO spectra taken at 88, 110, 130, 190, 210, 285, 500, and 900 eV. It is noticed that the PIPICO spectra were taken under the same condition for the spectra shown in Figure 3. The variation of the individual PIPICO yield with energy is presented in Figure 6. Quite similar energy dependence as observed for the

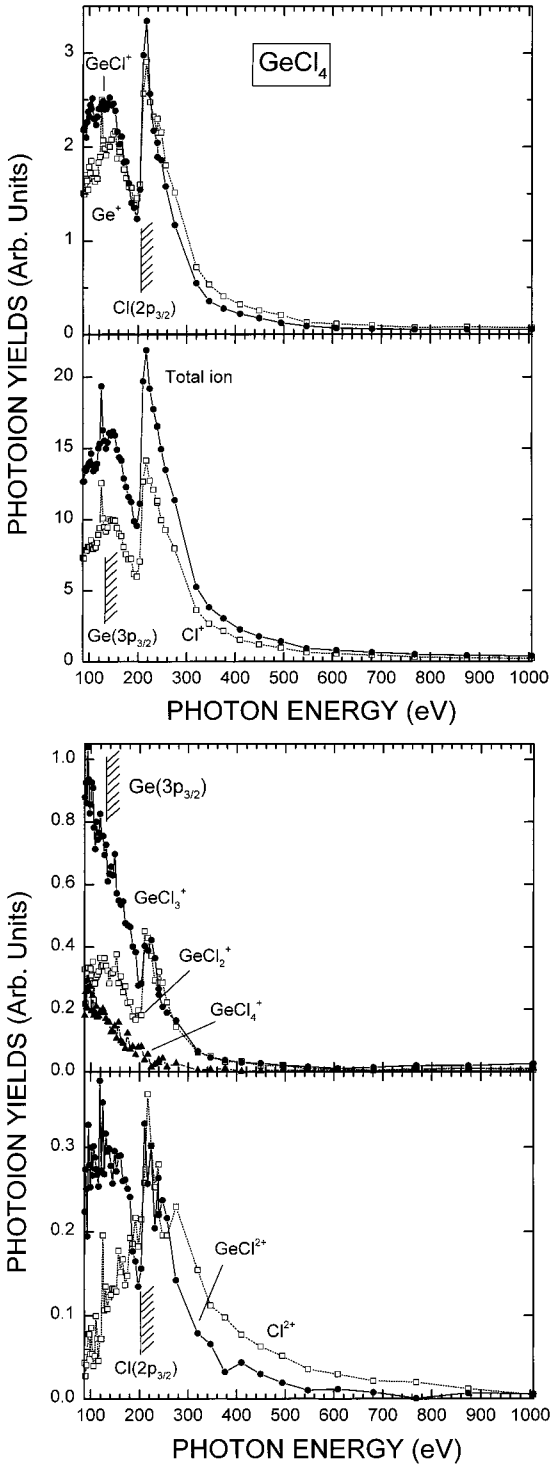


**Figure 4.** Partial ion yield spectra of $GeCl_4$. The spectral intensities ($I_{photoion}/I_{tot-photon}$) are presented on the same relative intensity scale.

individual ion yields is observed for the individual PIPICO yields. This indicates that the ions formed involve the results of dissociative multiple ionization. If single ionization prevails, the spectral shapes of the ion and PIPICO yield spectra should be quite different from each other. It is noticed again that sum of the individual PIPICO yields is equal to the total PIPICO yield as shown in Figure 2. At least five ion pairs of $Cl^+-Cl^+$, $Cl^+-Ge^+$, $Cl^+-GeCl^+$, $Cl^+-GeCl_2^+$, and $Cl^+-GeCl_3^+$ are visualized in the PIPICO spectra. It should be noticed that $Cl^+-Cl^+$ ion pair channel is not the result of Cl−Cl bond cleavage,

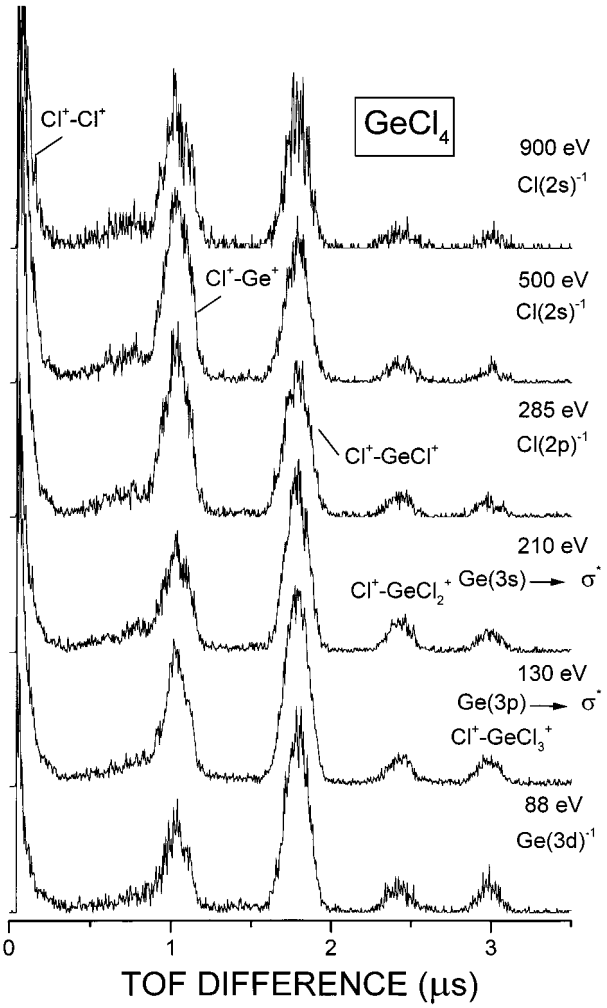


**Figure 5.** PIPICO spectra of $GeCl_4$ taken by excitations at photon energies at 88, 130, 190, 160, 210, 285, 500, and 900 eV. The deepest core orbitals, which could be excited/ionized by the specified energy, are marked in the individual spectra.

and thus $Ge^+$, $GeCl^+$, and $GeCl_2^+$ ions are probably involved as the third body in the ion pair formation of $Cl^+-Cl^+$. The PIPICO channels are given in the order of the increasing TOF difference. The most efficient process at 88 eV, the lowest energy examined here, is the ion pair formation of $Cl^+-GeCl^+$, accounting for 50% of the whole PIPICO channels (Figure 5). At this energy, the other channels $Cl^+-Ge^+$ and $Cl^+-Cl^+$ are also found to be competitive. Also the energy profile of the three PIPICO channels look similar to each other, as in the case that the energy profiles of the $Cl^+$, $Ge^+$, and $GeCl^+$ intensities are very similar. This can be taken as an indication that the three ions are the results of the similar reaction pathways. The possible reaction pathways involving the intermediacy of the $GeCl_4^{2+}$ doubly charged ion are outlined in Scheme 1.

**SCHEME 1**

$$
\begin{aligned}
GeCl_4 + h\nu &\rightarrow GeCl_4^{2+} + 2e \\
GeCl_4^{2+} &\rightarrow Cl^+ + Cl^+ + GeCl_2 \\
&\rightarrow Cl^+ + Ge^+ + 3Cl \text{ (or } Cl_2 + Cl) \\
&\rightarrow Cl^+ + GeCl^+ + 2Cl \text{ (or } Cl_2) \\
&\rightarrow Cl^+ + GeCl_2^+ + Cl \\
&\rightarrow Cl^+ + GeCl_3^+
\end{aligned}
$$

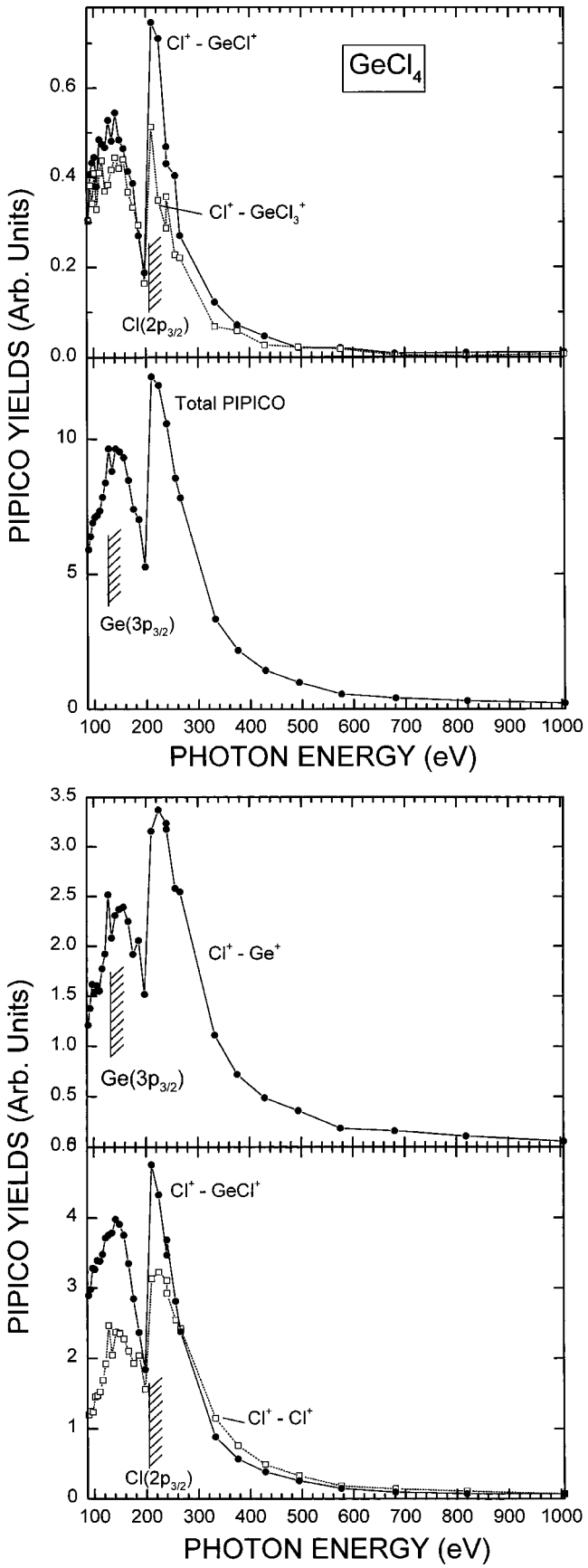


**Figure 6.** Individual PIPICO yield spectra of $GeCl_4$. The spectral intensities ($I_{PIPICO}/I_{tot-photon}$) are presented on the same relative intensity scale.

However, it is elucidated that such simple ion-pair formation outlined in Scheme 1 cannot account for the formation of the

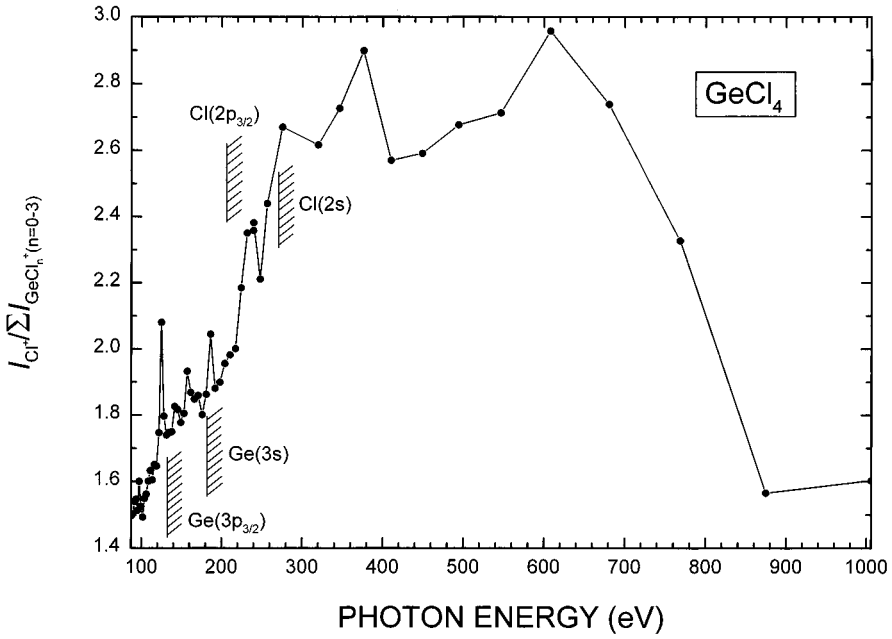


**Figure 7.** Ratios of integrated intensities of $Cl^+$ in the TOF spectra to the sum of the intensities of $GeCl_n^+$ ($n = 0-3$) [$I_{Cl^+}/\Sigma I_{GeCl_n^+(n=0-3)}$] in $GeCl_4$.

$Cl^+$ ion with 62 ± 3% among the total ion intensity in the whole range examined. It is useful to notify that our simple PIPICO method may not clarify the occurrence of triple and quadruple photoionization, but the method may hint its possibility by comparing the ion intensity ratios as a function of energy. In Figure 7, we present the variation of the ratio of the ion intensity for $Cl^+$ to sum of the intensities for $GeCl_n^+$ ($n = 0-3$) [$I_{Cl^+}/\Sigma I_{GeCl_n^+(n=0-3)}$] with the photon energy. In the whole energy, the average ratio is as high as 2.4 ± 0.4. For example, in the case that only the double ionization as shown in reactions 1 and 2 occurs, the ratio should become one.

$$GeCl_4^{2+} \rightarrow Cl^+ + GeCl^+ + NP \quad (1)$$

$$GeCl_4^{2+} \rightarrow Cl^+ + Ge^+ + Np \quad (2)$$

Here NP refers to unidentified neutral products. Above the Ge(3p) threshold, the ratio increases up to about 3 at ~600 eV, indicating that the triple and quadruple ionization presumably occurs to yield abundant chlorine ion as outlined in Scheme 2.

**SCHEME 2**

$$\begin{aligned} GeCl_4 + h\nu &\rightarrow GeCl_4^{3+} + 3e \\ GeCl_4^{3+} &\rightarrow Cl^+ + Cl^+ + GeCl^+ + Cl \\ &\rightarrow Cl^+ + Cl^+ + Ge^+ + 2Cl \\ GeCl_4 + h\nu &\rightarrow GeCl_4^{4+} + 4e \\ GeCl_4^{3+} &\rightarrow Cl^+ + Cl^+ + Cl^+ + GeCl^+ \\ &\rightarrow Cl^+ + Cl^+ + Cl^+ + Ge^+ + Cl \end{aligned}$$

Above the energy ≈600 eV, the ratio decreases rapidly, (Figure 7) implying that at the high energy, surprisingly the valence ionization may again play an important role in the photoionization, leading to only double and triple ionization of the molecule. This could occur when nonresonant valence ionization prevails. This interpretation is also supported by the observations that the $GeCl_n^+$ ($n = 1-3$) intensities rise, as seen Figure 3. In our simple PIPICO mode, however, it is impossible to detect three or more ions simultaneously. The formation of the ion pair $Cl^+-Cl^+$ hints at least the occurrence of triple ionization because the ionization potential of the chlorine atom is much larger than that of the germanium atom, the $Ge^+$ (or $GeCl^+$ or $GeCl_2^+$) ion is most likely formed along with the ion pairs of $Cl^+-Cl^+$. Apparently, any combination of the ion pairs in processes 3 and 4 is clearly detected in our PIPICO experiment.

$$GeCl_4^{3+} \rightarrow Cl^+ + Cl^+ + Ge^+ + 2Cl \quad (3)$$

$$GeCl_4^{3+} \rightarrow Cl^+ + Cl^+ + GeCl^+ + Cl \quad (4)$$

Therefore the dissociative triple ionization, processes 3 and 4 mainly contribute to the total PIPICO channel above the Cl(2p) threshold. The variation of the partial ion and PIPICO yields with energy is discussed in conjunction with the relevant electronic states, on the basis of the observations of the ion and PIPICO intensities as a function of energy.

**$Cl^{2+}$ Channel.** As seen in Figure 3, the $Cl^{2+}$ is observed significantly above the Cl(2s) threshold. However, the PIPICO channel involving the doubly charged ion was not detected due probably to the low intensity. The formation of the $Cl^{2+}$ ion in lesser amount even in the Cl(2p) region indicates that charge redistribution in the whole molecule occurs rapidly prior to bond cleavage followed by the local Auger process.

**$Cl^+$ Channel.** As seen in Figures 5 and 6, the PIPICO intensities of the $Cl^+-GeCl^+$ and $Cl^+-Ge^+$ channels are mutually compensated, indicating the $Cl^+-Ge^+$ channel is more or less the result of the depletion of the $GeCl^+$ channel due to process 5.

$$GeCl^+ \rightarrow Cl^+ + Ge \quad (5)$$

**$GeCl^{2+}$ Channel.** The $GeCl^{2+}$ ion is the only one doubly charged molecular ion detected in the $GeCl_4$ system. However, the intensity is too low for the detection of the PIPICO experiment. The intensity is almost invariant with energy, implying that the doubly charged ion is the result of the nonresonant valence ionization.

**$GeCl_n^+$ (0−4) Channels.** The yield ratio for the $GeCl_n^+$ ($n = 1-4$) ion decreases with increasing the photon energy up to ~600 eV, from which the yield ratios rises slowly, indicating that at the high energy above 600 eV, valence ionization prevails and thus heavy ions of $GeCl_n^+$ ($n = 3-4$) are significantly abundant (Figure 3). The intensities of the $Ge^+$ and $GeCl^+$ ions account for 77 ± 5% of the total germanium-containing ions, demonstrating that the three or all four ligands were eliminated as singly charged ions from the molecular ion upon the VUV irradiation to the molecules. As seen in Figure 4, the $GeCl_4^+$ ion yield decreases with increasing the energy, not specifically showing the Ge(3p) and Cl(2p) strong features. This presumably indicates that the formation of the parent ion partially involves the result of the nonresonant valence ionization because the $GeCl_4^+$ ion corresponds to only the loss of one electron and the electron ejection from the core level of the $GeCl_4$ molecule leads to further fragmentation of the parent ion. But the probability of the nonresonant single ionization yielding the $GeCl_4^+$ ion is found to be very small.

## Conclusions

Specific fragmentation processes following the Ge(3d,3p,-3s) and Cl(2p,2s) inner-shell regions of $GeCl_4$ have been investigated in the range of 88−1006 eV by means of the PEPICO and PIPICO methods coupled to synchrotron radiation. Here we have observed discrete doublet features below the $Ge(3p_{3/2})$ threshold corresponding to the excitation of the $Ge(3p_{3/2})$ and $Ge(3p_{1/2})$ to the $\sigma(a_1)^*$ antibonding orbital. The broad and prominent feature noted C above the $Cl(2p_{3/2}) = 206.7$ eV can be identified as overlapped numerous discrete resonances corresponding to the transitions of the inner-shell orbitals, the $Cl(2p_{3/2})$ and $Cl(2p_{1/2})$ to the $\sigma^*$ valence orbitals, and the $n$s and $n$p Rydberg series. The shoulder peak spanning the Cl(2s) threshold and about 500 eV may correspond to a shape resonance, arising from the cage effect caused by the potential barrier created by the four electronegative chlorine ligands. The formation of the $Cl^{2+}$ ion in lesser amount even in the Cl(2p) region indicates that charge redistribution occurs rapidly, prior to bond cleavage followed by the subsequent local Auger process. The triple and quadruple photoionization of $GeCl_4$ is found to dominantly occur in the Cl(2p) and Cl(2s) excitation regions, giving rise to the exclusive formation of the $GeCl_n^+$ ($n = 0, 1$) + $nCl^+$ ($n = 2-3$) channels.

**Acknowledgment.** The authors acknowledge the financial support of the Korea Research Foundation through the Non-Directed research program of 1998−1999. The staffs of the accelerator group of the Electrotechnical Laboratory in Tsukuba, Japan, are greatly acknowledged for the use of the synchrotron radiation facility.

## References and Notes

(1) Hitchcock, A. P. *J. Electron Spectrosc. Relat. Phenom.* **1982**, *25*, 245.
(2) Eland, J. H. D. In *Vacuum Ultraviolet Photoionization and Photodissociation of Molecules and Clusters*; Ng, C. Y., Ed.; World Scientific: Singapore, 1991; p 297, and references therein.
(3) Eland, J. H. D. *Mol. Phys.* **1987**, *61*, 725.
(4) Hsieh, S.; Eland, J. H. D. *J. Phys. B: At. Mol. Opt. Phys.* **1997**, *30*, 4515.
(5) Nenner, I.; Morin, P. In *VUV and Soft X-ray Photoionization*; Becker, U., Shirley, D. A., Eds.; Plenum: New York, 1996; p 291.
(6) Hsieh, S.; Eland, J. H. D. *Rapid Commun. Mass Spectrom.* **1995**, *9*, 1261.
(7) Ninomiya, K.; Ishiguro, E.; Iwata, S.; Mikuni, A.; Sasaki, T. *J. Phys. B* **1981**, *14*, 1777.
(8) Fronzoni, G.; Stener, M.; Decleva, P.; De Alti, G. *Chem. Phys.* **1998**, *232*, 9.
(9) Zhang, W.; Ibuke, T.; Brion, C. E. *Chem. Phys.* **1992**, *160*, 435.
(10) Au, J. W.; Brion, C. E. *Chem. Phys.* **1997**, *218*, 87.
(11) Guillot, F.; Dézarnaud-Dandine, C.; Tronc, M.; Modelli, A.; Lisini, A.; Decleva, P.; Fronzoni, G. *Chem. Phys.* **1996**, *205*, 359.
(12) Guillot, F.; Dézarnaud-Dandine, C.; Tronc, M. *Chem. Phys.* **1997**, *224*, 281.
(13) Caldwell, C. D.; Krause, M. O.; Cowan. R. D.; Menzel, A.; Whitfield, S. B.; Hallman, S.; Frigo, S. P.; Severson, M. C. *Phys. Rev. A* **1999**, *59*, R926.
(14) Martins, M. *J. Phys. B: At. Mol. Opt. Phys.* **2001**, *34*, 1321.
(15) Dehmer, J. L. *J. Chem. Phys.* **1971**, *56*, 4496.
(16) Sze, K. H.; Brion, C. E. *Chem. Phys.* **1989**, *137*, 353.
(17) Saito, N.; Suzuki, I. H. *Int. J. Mass Spectrom. Ion Process.* **1988**, *82*, 61.
(18) Saito, N.; Suzuki, I. H. *Int. J. Mass Spectrom. Ion Process.* **1992**, *115*, 157.
(19) Henke, B. L. *Nucl. Instrum. Meth.* **1980**, *177*, 161.
(20) Drake, J. E.; Riddle, C.; Coatsworth, L. *Can. J. Chem.* **1975**, *53*, 3602.
(21) Bakke, A. A.; Chen, H.-W.; Jolly, W. L. *J. Electron Spectrosc. Relat. Phenom.* **1980**, *20*, 333.
(22) Perry, W. B.; Jolly, W. L. *Inorg. Chem.* **1974**, *13*, 1211.
(23) Bearden, J. A.; Burr, A. F. *Rev. Mod. Phys.* **1967**, *39*, 125.
(24) Boo, B. H.; Saito, N.; Suzuki, I. H.; Koyano, I. *J. Mol. Struct.* **2002**, in press.
(25) Hayes, W.; Brown, F. C.; Kunz, A. B. *Phy. Rev. Lett.* **1971**, *27*, 774.